Identifying the coiled-coil triple helix structure of β-peptide nanofibers at atomic resolution

Article (Accepted Version)

Article

Identifying the Coiled-Coil Triple Helix Structure of #-Peptide Nanofibers at Atomic Resolution

Andrew J. Christofferson, Zahraa S Al-Garawi, Nevena Todorova, Jack Turner, Mark Pasqualino Del Borgo, Louise C. Serpell, Marie-Isabel Aguilar, and Irene Yarovsky

ACS Nano, **Just Accepted Manuscript** • Publication Date (Web): 29 Aug 2018

Identifying the Coiled-Coil Triple Helix Structure of β-Peptide Nanofibers at Atomic Resolution

Andrew J. Christofferson,[a‡] Zahraa S. Al-Garawi,[bc‡] Nevena Todorova,[a] Jack Turner,[b] Mark P. Del Borgo,[d] Louise C. Serpell,[b] Marie-Isabel Aguilar,[d*] and Irene Yarovsky[a*]*

[a] School of Engineering, RMIT University, Melbourne, VIC 3001, Australia. E-mail: irene.yarovsky@rmit.edu.au

[b] School of Life Sciences, University of Sussex, Falmer, East Sussex BN1 9QG, UK. E-mail: l.c.serpell@sussex.ac.uk

[c] Chemistry Department, Mustansiriyah University, Baghdad, Iraq.

[d] Department of Biochemistry and Molecular Biology and Biomedicine Discovery Institute, Monash University, Melbourne, VIC 3800, Australia. E-mail: mibel.aguilar@monash.edu

KEYWORDS: beta-peptides • nanostructured materials • self-assembly • structure elucidation • supramolecular chemistry

ABSTRACT: Peptide self-assembly represents a powerful bottom-up approach to the fabrication of nanomaterials. β^3-peptides are non-natural peptides composed entirely of β-amino acids, which have an extra methylene in the backbone and we reported fibers derived from the self-assembly of β^3-peptides that adopt 14-helical structures. β^3-peptide assemblies represent a class of stable nanomaterials that can be used to generate bio- and magneto-responsive materials with proteolytic stability. However, the three-dimensional structure of many of these materials remains unknown. In order to develop structure-based criteria for the design of β^3-peptide-based biomaterials with tailored function, we investigated the structure of a tri-β^3-peptide nanoassembly by molecular dynamics simulations and X-ray fiber diffraction analysis. Diffraction data was collected from aligned fibrils formed by Ac-β^3[LIA] in water and used to inform and validate the model structure. Models with threefold radial symmetry resulted in stable fibers with a triple-helical coiled-coil motif and measurable helical pitch and periodicity. The fiber models revealed a hydrophobic core and twist along the fiber axis arising from a maximization of contacts between hydrophobic groups of adjacent tripeptides on the solvent-exposed fiber surface. These atomic structures of macro-scale fibers derived from β^3-peptide-based materials provide valuable insight into the effects of the geometric placement of the side-chains and the influence of solvent on the core fiber structure which is perpetuated in the superstructure morphology.

Supramolecular self-assembly of peptides represents a powerful avenue to the bottom-up nanofabrication of next-generation functional materials and devices with tailored chemical and physical attributes. The self-assembly of peptides comprising α-amino acids that adopt α-helical and β-sheet structures has led to a wide range of peptide-based materials with particular applications in tissue engineering.[1-3] However, there are significant challenges in the longer-term application of these materials due to the difficulties in chemical functionalization (as the α-amino acid side chains are often involved in the self-assembly process) and proteolytic degradation. Peptides consisting of only β^3-amino acids, also known as β-peptides, are a class of foldamers which have an intrinsic propensity to form stable, well-defined secondary or tertiary structures, even from short tri-β^3-peptides.[4-7] The peptide monomers spontaneously self-assemble in a head-to-tail fashion which is driven by a 3-point hydrogen-bonding motif associated with the 14-helical structure of *N*-acetyl-β^3-peptides.[8] The 14-helical N-acetylated β^3-peptides studied self-assembled irrespective of the monomer sequence, and can therefore be modified with specific functional groups without affecting their ability to form fibers. Assemblies of β^3-peptide 14-helices, which take their name from the number of atoms in the hydrogen-bonded ring,[9,10] have been described previously for larger peptides, such as 10-residue β-peptides that form water-soluble aggregates in the range of tetramers to hexamers.[11] Schepartz *et al.* found that for β-peptides of seven to 11 monomer units, potential for association and stability of the 14-helix in water depended strongly on the peptide sequence,[12] and in 2007 successfully resolved the X-ray crystal structure of a homo-octamer of the 14-helix β-dodecapeptide Zwit-1F.[13] Müller *et al.* found that both sequence and N-terminal capping had a strong effect on self-assembly for β-decapeptides in aqueous solution.[14]

Since β-peptides are non-natural polymers and also exhibit high metabolic and mechanical stability, by exploiting the ability of these peptides to assemble into supramolecular entities, β-peptides represent a versatile class of functional nano- and biomaterials.[8,15-18] We have previously demonstrated that these fibers were able to bundle into hierarchical superstructures, providing an avenue for the development of bio- and nanomaterials,[15,17,19] including the functionalization of β^3-peptides with biological motifs and tuning the biological signal by the co-assembly of β^3-[LIA] to generate a hybrid 2D bioscaffold.[19,20] This bottom-up design template is extremely powerful as the behavior and function of the interfaces are "built-in" to the small peptide building blocks *via* the constituent β-amino acids, which manifest functionality when self-assembled into fibers. The effect of β^3-amino acid sequence on the superstructure of three isomeric β-peptides, Ac-β^3[LIA], Ac-β^3[IAL], and Ac-β^3[ALI],[21] was also examined and showed noticeably different superstructures for the three peptides by AFM, while far-infrared spectroscopy indicated similarity of the core structures, and that in water the carboxyl group was solvated in the assemblies. In separate studies it was further demonstrated that the physicochemical properties of the solvent have a strong effect on the lateral association of the nanorods which leads to superstructures of diverse geometries (Table 1).[8,21,22] These studies demonstrate that spatial distribution of different non-polar side chains and the solvent play a subtle yet important role in the self-assembly of these small molecules, which in turn impose fundamentally different structural characteristics on the resulting self-assembled nanomaterials. Despite the advancements in high-resolution imaging methods and microscopy techniques, characterization of the atomic structural features of these supramolecular self-assembled β-peptide systems remains a challenge. Development of structure-based criteria is essential for the

design of stable β^3-peptide nanomaterials with tailored function and to allow full exploitation of this bottom-up approach to the fabrication of peptide-based materials.

Table 1. Experimental morphology of stable Ac-β^3 tripeptides in polar protic, polar aprotic, and nonpolar solvents.

Solvent	Ac-β^3[LIA]	Ac-β^3[ALI]	Ac-β^3[IAL]
Water/ methanol	Large thick bundles[8,21,22]	Thin dendritic fibers[22]	Non-aligned fiber mesh[22]
Ethanol	Dendritic[21,22]	Dendritic[22]	2D structures[22]
2-Propanol	Dendritic[21,22]	Dendritic[22]	Dendritic[22]
Acetone	Straight short fibers[21]		
Chloroform	Straight short fibers[21]		

Over the last two decades, MD simulations have successfully sampled the conformational landscape of β-peptides and predicted different secondary structures for β-peptide monomers, including the 3_{14}-helix,[23-25] 2.5_{12}-helix,[26] $2.7_{10/12}$-helix,[25,27] hairpin structure,[28] structures with cyclic side-chains,[29] and have shown the effects of solvents at various levels of detail.[29-31] More recently, theoretical and computational methods have also proven to be a powerful tool in the investigation and modulation of intermolecular, noncovalent interactions between self-assembling peptides or proteins in solution to produce materials with predetermined motifs[32] and morphologies, including desired symmetries.[33,34]

Much work has been done on the computational design and characterization of β-peptide assemblies. In 2002, the group of DeGrado *et al.* used molecular mechanics to design a 14-helix

β^3-peptide with enhanced helix-helix interactions when the two helices were connected by a disulfide bond.[35] Following their development of a computational approach for the design of computed helical anti-membrane protein (CHAMP),[36] the DeGrado group utilized computational and experimental methods to determine the characteristic IR signature of 14-helix β-peptides[37] and develop a rotamer library for β-peptide backbones,[38] culminating in the release of the Non-natural Automated Protein or Ligand (NAPOLI) platform[39] and the computational design of the membrane-targeting 14-helix β-peptide β-CHAMP.[40] In their atomistic studies of β-peptide association, the Yethiraj group found that peptide sequence has a strong effect on the orientational order of β-peptide self-assembled monolayers,[41] self-assembly of dimers and trimers,[42] and pKa shifts in the β-peptide side chains.[43] They also found that amphiphilic β-peptide aggregation is driven by entropy or energy, depending on the solvent.[44] In a series of coarse-grained (CG) studies, the Yethiraj group were able to fit a CG model and theoretical structure factor to small-angle X-ray scattering data to characterize the nanostructure of β-peptide assemblies,[45] and found that at the CG level of theory, aggregation, fiber stability, and self-assembly of micelles also depended strongly on the peptide sequence.[46,47] In their series of studies on β-peptide structure and association, the De Pablo group used potential of mean force to examine the relative stability of the 12- and 14-helices in implicit and explicit solvents,[48,49] and found that entropic effects play a role in the stability of β-peptides in explicit water, and the helical folded structure is due to balance between intra-peptide interactions and water-mediated interactions.[50] They also found a decrease in hydrophobic solvent-accessible surface area in explicit solvent, and upon dimerization.[51] To explore the interaction landscape of these peptides further, they applied metadynamics to obtain the multidimensional free energy of dimerization, which showed that β-peptides can exhibit a variety of interactions, dependent on orientation,

which elucidate the behavior seen experimentally.[52] Overall, these studies have largely focused on monomers or bundles of 2-8 monomers, or coarse-grained assemblies, and to date there are no reports focused on the atomistic computational modelling of β^3-tripeptide-containing nanofibers.

Despite intensive research, the atomic-level characteristics of full β-peptide nanofibers have never been elucidated. While several tools exist for the construction of helices and coiled coils of α-L-amino acids, such as YASARA,[53] MODELLER,[54] CC Builder,[55] and the NAPOLI platform for non-natural peptides,[39] to the best of our knowledge nothing has been developed for the construction and assembly of β^3-peptide coils where there is not a continuous covalent backbone along the fiber axis. We have therefore developed a systematic and sequence-independent procedure for the modeling of β^3-peptide helices, following a protocol similar to our previous studies of cyclic[56] and linear[57] triple helices of poly(methyl methacrylate), as well as coiled-coil standard α-L-amino acids.[58] Specifically, we employed explicit atomistic solvent MD simulations to investigate the core nano-fiber structures of the *N*-acetylated tri-β^3-peptides Ac-β^3[LIA], Ac-β^3[IAL] and Ac-β^3[ALI], in polar protic, polar aprotic, and nonpolar solvents. Detailed X-ray fiber diffraction data was collected from aligned fibrils formed by Ac-β^3[LIA] in water and used to validate the model structure. The resultant structures provide insight into how side-chain geometric placement and solvent physicochemical properties influence the core fiber structure of a full β-peptide fiber, which consequently affect the fibers' superstructure morphology.

RESULTS

Assembly of Ac-β^3[LIA] in water. Electron microscopy was used to examine the morphology of the fibers formed by self-assembled Ac-β^3[LIA] in water after three days incubation at 1mg/ml. The peptide formed flat tapes with varied widths of 64-108 nm and helical tubes (67-80 nm) consistent with our previous AFM analyses[21] (Figure 1a, Figure S1, Supporting Information).

X-ray fiber diffraction from Ac-β^3[LIA]. An X-ray fiber diffraction pattern was collected from a partially aligned fiber bundle of self-assembled Ac-β^3[LIA]. The well-oriented diffraction pattern showed a series of sharp diffraction signals on the meridian and equatorial direction arising from the repeating structure within the aligned fibrils (Fig 1b). A strong meridional signal was observed at ~5 Å and weaker signal at 4.74 Å. These signals arise from the repeating units along the vertical fiber axis. A strong equatorial diffraction signal was observed beside the backstop at approximately 30 Å and further equatorials were observed at 14.5 Å, 11.1 Å and 7.23 Å, arising from the width of the molecules and their lateral packing within the architecture of the fiber bundle. This fiber X-ray diffraction pattern was then used to inform and validate the model structure.

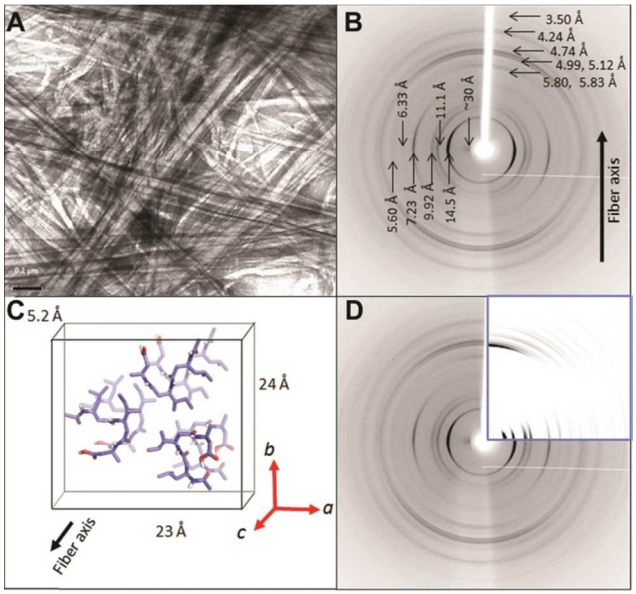

Figure 1. Structural characterization and validation of Ac-β^3[LIA] fibers formed in water. A) Electron micrograph showing highly ordered, straight tapes and tubes formed after three days incubation (1mg/ml in H_2O at 37 °C); B) X-ray fiber diffraction pattern from aligned fibers; C) modeled coordinates of a potential unit cell where *c* corresponds to the H-bonding of amide groups along the fiber axis; D) experimental diffraction pattern overlaid with the diffraction pattern calculated from the model shown in C) (insert outlined in blue).

Structural modeling of an Ac-β^3[LIA] fiber in water. As the timescales for the self-assembly of full β-peptide nanofibers are beyond the reach of current atomistic simulation techniques, we constructed a series of model fiber configurations and allowed the well-parameterized molecular mechanics force field to relax the structures by molecular dynamics simulations in explicit solvent, which were then compared to the fiber X-ray diffraction data. Because isoleucine is the most hydrophobic of the three residues,[59] initial fiber cross-sections of three to six Ac-β^3[LIA] peptides were constructed with the isoleucines forming a hydrophobic core. Cross-sections of threefold, fourfold, and fivefold radial symmetry were arranged with the isoleucines in hydrophobic contact (~4 Å) of the adjacent isoleucine, while for the six-fold radial symmetry the closest contact that could accommodate six tripeptides was ~6 Å (Figure S2,

Supporting Information). Cores formed by leucine and combinations of isoleucine and leucine were also tested, as well as parallel and antiparallel arrangements and N-terminal acetyl capping.

Of the four initial radial geometries, only structures with a threefold radial symmetry, parallel alignment, N-terminal acetyl capping, and isoleucine in the hydrophobic core resulted in stable fibers. These fibers exhibited a measurable helical pitch and periodicity of 152 ± 18 Å and 33 ± 4 tripeptides per turn, respectively. These fibers formed a triple helical coiled coil motif, characterized by a hydrophobic core of isoleucines, with the twist along the fiber axis arising from a maximization of contacts between the leucines and alanines of adjacent tripeptides on the solvent-exposed surface of the fiber (Figure 2A, Figure S3, Supporting Information).

A single layer of the model generated with three subunits was arranged in a unit cell with dimensions a=23 Å, b=24 Å, c= 5.2 Å, α=β=γ=90° (Figure 1C) and CLEARER[60] was used to calculate a fiber diffraction pattern in which c corresponds to the fiber axis. Comparison with the experimental data shows an exceptional match at all diffraction signal positions except at the strong reflection 24 Å which arises from the edge of the unit cell (Figure 1D). Significantly, model cross-sections with other than threefold radial symmetry failed to reproduce the experimental diffraction signals (Figure S4, Supporting Information).

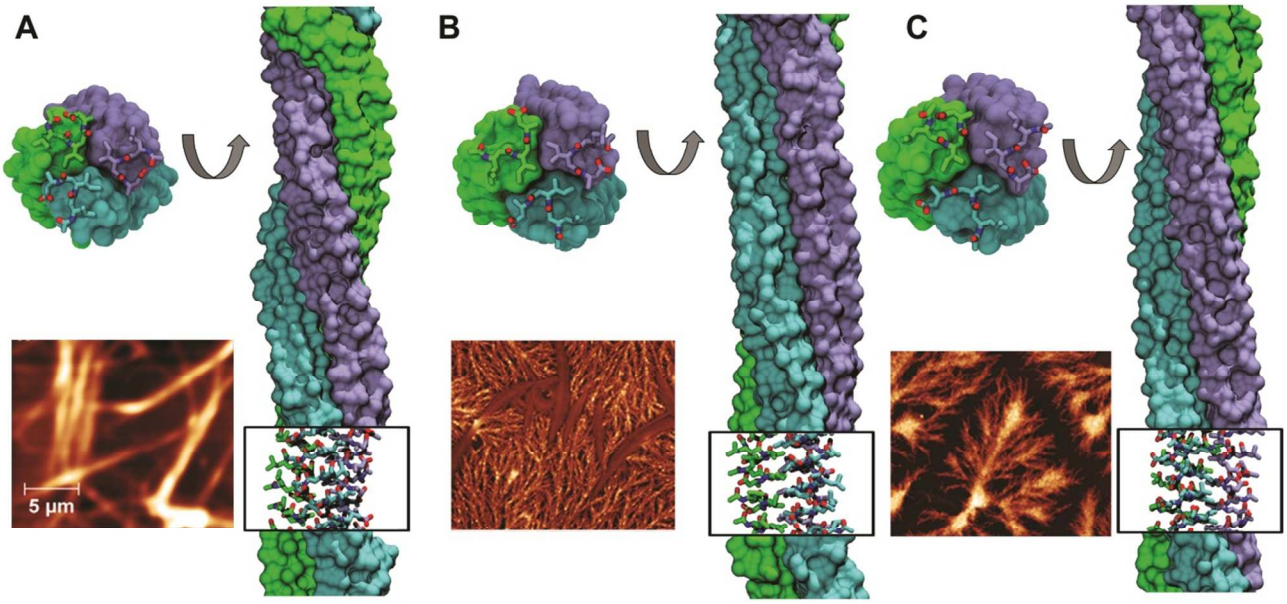

Figure 2. Model structures of Ac-β^3[LIA] in A) water, B) ethanol, and C) 2-propanol, with corresponding AFM images. Oxygens are colored red, nitrogens blue, and the carbons of the three individual strands that make up the fiber are colored green, purple, and cyan, respectively. Solvent molecules and hydrogen atoms are not shown for clarity. AFM images reproduced and adapted from Reference 22 with permission.

Structure of Ac-β^3[LIA] fibers in other solvents. Further molecular dynamics simulations were conducted to explore the effect of solvent on the Ac-β^3[LIA] fiber structure. An increase in the helical pitch (Table 2) was observed as the solvent was changed from water (152 ± 18 Å with 33 ± 4 tripeptides per turn - Figure 2A) to ethanol (217 ± 24 Å with 46 ± 5 tripeptides per turn - Figure 2B) to 2-propanol (227 ± 23 Å with 48 ± 5 tripeptides per turn - Figure 2C), corresponding to a decrease in interactions between leucines and alanines of adjacent tripeptides on the solvent-exposed surface of the fiber (Figure 2 and Figure S5, Supporting Information). It was previously observed experimentally that Ac-β^3[LIA] formed dendritic structures in ethanol and 2-propanol but not in water,[22] and this may be due to the fact that a more open helix with

fewer lateral intra-fiber interactions is more available for branching and association with free Ac-β^3[LIA] peptide monomers in solution.

In chloroform, the three individual strands of the isoleucine-core model separated, but the hydrogen bonds along the axis of the strands remained intact, resulting in three isolated linear strands with few inter-strand interactions. A model with the terminal carboxyl groups in the core was therefore constructed, which remained stable in chloroform (673 ± 112 Å with 140 ± 23 tripeptides per turn - Figure 3). Results with acetone were similar to those with chloroform (557 ± 94 Å with 115 ± 19 tripeptides per turn - Figure S5, Table 2), with the isoleucine-core model dissolving and the carboxyl-core model remaining stable. Experimentally, the Ac-β^3[LIA] peptides formed short, straight fibers in both chloroform and acetone.[21]

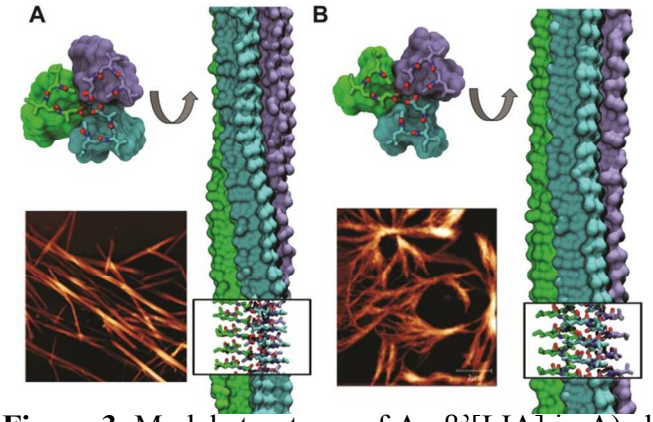

Figure 3. Model structures of Ac-β³[LIA] in A) chloroform, and B) acetone, with corresponding The three individual strands that make up the fiber are colored green, purple, and cyan, respectively. Solvent molecules and hydrogen atoms are not shown for clarity. AFM images reproduced and adapted from Reference 21 with permission from the Royal Society of Chemistry.

Table 2. Characteristics of stable Ac-β^3-tripeptides in polar protic, polar aprotic, and nonpolar solvents.

	Water	Ethanol	2-propanol	Acetone	Chloroform
LIA					
Helical pitch (Å)	152 ± 18	217 ± 24	227 ± 23	557 ± 94	673 ± 112
Tripeptides per turn	33 ± 4	46 ± 5	48 ± 5	115 ± 19	140 ± 23
Fiber diameter (Å)	15.66 ± 0.09	15.66 ± 0.08	15.70 ± 0.10	15.49 ± 0.08	15.44 ± 0.08
Backbone H-bonds[a]	60 ± 5 %	67 ± 5 %	67 ± 5 %	76 ± 5 %	75 ± 5 %
SASA[b] (Å²)	5726 ± 125	6017 ± 118	6077 ± 124	6315 ± 103	6129 ± 97
Contact area[c] (Å²)	1076 ± 25	1051 ± 20	1033 ± 20	937 ± 25	932 ± 28
ALI					
Helical pitch (Å)	150 ± 11	146 ± 23	206 ± 47		
Tripeptides per turn	31 ± 2	32 ± 4	43 ± 9		
Fiber diameter (Å)	16.42 ± 0.13	17.48 ± 0.39	16.96 ± 0.49		
Backbone H-bonds[a]	69 ± 5 %	73 ± 5 %	72 ± 5%		
SASA[b] (Å²)	6033 ± 160	6624 ± 248	6613 ± 215		
Contact area[c] (Å²)	1173 ± 30	1024 ± 59	1076 ± 42		
IAL					
Helical pitch (Å)	151 ± 21	303 ± 39	301 ± 51		
Tripeptides per turn	32 ± 5	64 ± 8	63 ± 10		
Fiber diameter (Å)	16.00 ± 0.15	16.63 ± 0.17	16.70 ± 0.16		
Backbone H-bonds[a]	65 ± 5 %	75 ± 5 %	75 ± 5 %		
SASA[b] (Å²)	5786 ± 155	6423 ± 132	6459 ± 133		
Contact area[c] (Å²)	1264 ± 31	1152 ± 29	1144 ± 29		

[a] Percentage of possible backbone hydrogen bonds in the core that are occupied on average.

[b] Solvent-accessible surface area of the fiber core, excluding the cross-sections.

[c] Contact area between a single strand in the fiber core and the two adjacent strands

Structure of Ac-β^3[ALI] fibers in water and alcohols. For the second peptide, Ac-β^3[ALI], the isoleucine is directly adjacent to the C-terminal carboxylic acid and cross-sections constructed with the isoleucines in the core also place the carboxyl group in the core, which failed to produce stable fibers. Subsequently, we built cross-sections with the leucines forming the core. These still failed to produce stable structures until we rotated the C-terminal backbone in order to place the isoleucine adjacent to the alanine of the same tripeptide monomer (Figure 4A, Figure S3, Supporting Information). The resultant Ac-β^3[ALI] fiber has a helical pitch of 150 ± 11 Å with 31 ± 2 tripeptides per turn, similar to the Ac-β^3[LIA] fiber (Table 2), but a far more open face, demonstrated by the increase in solvent-accessible surface area, compared to the tightly-wrapped Ac-β^3[LIA]. The Ac-β^3[ALI] fiber also exhibited defects along the outside of the fiber (Figure 4C, red circles). The Ac-β^3[ALI] peptide is the only peptide to produce dendritic structures in all of the solvents studied,[22] and this may be due to these defects, which can serve as branching points for the fiber. Similar to the Ac-β^3[LIA] fiber, the decrease in solvent dielectric constant corresponded to an increase in helical pitch, a decrease in side-chain contacts on the fiber surface (Figure S6, Supporting Information), as well as an increase in the number of defects.

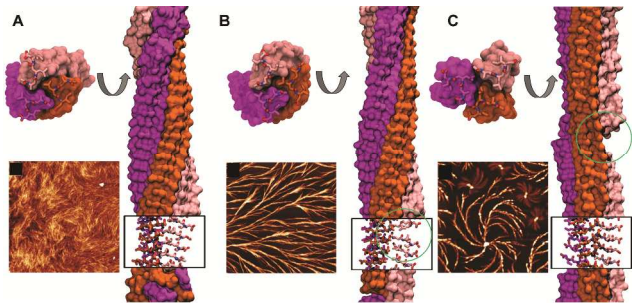

Figure 4. Model structures of Ac-β[3][ALI] in A) water, B) ethanol, and C) 2-propanol, with corresponding AFM images. Oxygens are colored red, nitrogens blue, and the carbons of the three individual strands that make up the fiber are colored pink, purple, and orange, respectively. Solvent molecules and hydrogen atoms are not shown for clarity. Fiber defects are circled in green. AFM images reproduced and adapted from Reference 22 with permission.

Structure of Ac-β[3][IAL] fibers in water and alcohols. Initial fiber cross-sections of the third peptide, Ac-β[3][IAL], were constructed in a similar fashion to Ac-β[3][LIA], with the isoleucines forming a hydrophobic core. However, during simulation the fibers spontaneously reorganized to a slightly different cross-sectional configuration (Figure 5A, Figure S3, Supporting Information), with the core formed by a single isoleucine. In this structure, the isoleucine in each tripeptide of the cross-section is found in a different chemical environment, with the core isoleucine in hydrophobic contact with the adjacent leucine and alanine of one peptide, and the alanine of the other adjacent peptide. For the remaining two isoleucines, one is in hydrophobic contact with the adjacent alanine, and the other in contact with the adjacent leucine. This irregularity could disfavor ordered hierarchical aggregation and may be the reason for the mesh of non-aligned fibers observed experimentally.[22] Despite these differences in core structure, the fiber has the same approximate helical pitch (151 ± 21 Å, 32 ± 5 tripeptides per turn) as the Ac-β[3][LIA] fiber.

In ethanol, the Ac-β^3[IAL] fiber exhibits a much more ordered arrangement with curvature but far less consistent twist along the fiber axis. This corresponds to the 2D structures observed experimentally.[22] In 2-propanol, the fiber is much more ordered, and begins to resemble the more open Ac-β^3[ALI] fiber. The Ac-β^3[IAL] fiber only forms dendritic structures in 2-propanol.[22]

Structure of Ac-β^3[AIL], Ac-β^3[ILA], and Ac-β^3[LAI] fibers in water. Initial fiber cross-sections of these Ac-β^3-tripeptides were generated from cross-sections of their stable isomers Ac-β^3[LIA], Ac-β^3[ALI], and Ac-β^3[IAL], respectively, with the first and third residues exchanged. While these Ac-β^3-tripeptides have not been synthesized experimentally, they all formed stable fibers with core structures broadly similar to their analogues containing the same middle residue (Figure S3, Supporting Information).

Comparison between structural characteristics and experimental morphology. A comparison between the characteristics of the model structures of each and their experimental morphology from AFM is presented in Table 3. In general, a decrease in dielectric constant was associated with 1) an increase in helical pitch and units per turn, 2) an increase in backbone stability as described by backbone hydrogen bonds, 3) an increase in solvent-accessible surface area, and 4) a decrease in contact area between adjacent strands (Table 2). For polar protic solvents, the decrease in dielectric constant from water to 2-propanol is also associated with an increase in structural defects, which may serve as branching points for the dendritic fibers. In polar aprotic and nonpolar solvents, the fiber core is formed by carboxyl groups and there is minimal periodicity which experimentally corresponds to short straight fibers. Overall, while all *N*-acetylated β-peptides adopt a 14-helix and self-assemble irrespective of amino acid sequence, the results clearly show that the influence of small changes in either the sequence or the solvent environment on fiber morphology can be modeled using the methods established here.

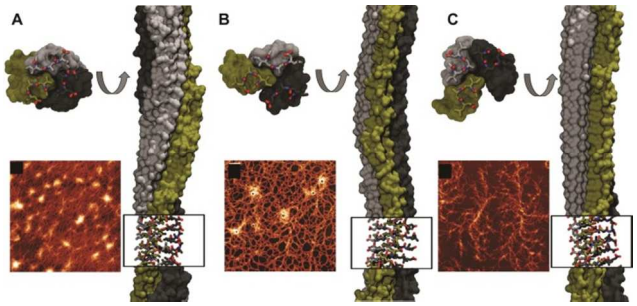

Figure 5. Model structures of Ac-β^3[IAL] in A) water, B) ethanol, and C) 2-propanol, with corresponding AFM images. Oxygens are colored red, nitrogens blue, and the carbons of the three individual strands that make up the fiber are colored gold, grey, and black, respectively. Solvent molecules and hydrogen atoms are not shown for clarity. AFM images reproduced and adapted from Reference 22 with permission.

Table 3. Comparison between structural characteristics and experimental morphology of stable Ac-β^3 tripeptides in polar protic, polar aprotic, and nonpolar solvents.

Solvent	Ac-β^3[LIA]	Ac-β^3[ALI]	Ac-β^3[IAL]
Water/ methanol			
Model	Regular, compact triple helix with Ile core	Less compact triple helix with Leu core	Irregular triple helix with Ile core
Experiment	*Large thick bundles*[8,21,22]	*Thin dendritic fibers*[22]	*Non-aligned fiber mesh*[22]
Ethanol			
Model	Increased helical pitch relative to water structure	Increased helical pitch and more defects relative to water structure	Increased regularity relative to water structure
Experiment	*Dendritic*[21,22]	*Dendritic*[22]	*2D structures*[22]
2-Propanol			
Model	Increased helical pitch relative to ethanol structure, some defects	Increased helical pitch and more defects relative to ethanol structure	Increased regularity relative to ethanol structure, more open helix, some defects
Experiment	*Dendritic*[21,22]	*Dendritic*[22]	*Dendritic*[22]
Acetone			
Model	Straight fibers with carboxyl core		
Experiment	*Straight short fibers*[21]		
Chloroform			
Model	Straight fibers with carboxyl core		
Experiment	*Straight short fibers*[21]		

CONCLUSIONS

In summary, we have described the structural model for a stable three-stranded helical coiled coil for self-assembled *N*-acetyl-β^3-peptides using X-ray fiber diffraction and molecular dynamics simulations. These 14-helical structures are distinct from α-peptide helical structures, with approximately three residues per turn and self-assembly is mediated by a head-to-tail H-bonding motif. The triple 14-helical coiled coil motif is characterized by a strongly hydrophobic core with the twist along the fiber axis arising from a maximization of contacts between the leucines and alanines of adjacent tripeptides on the solvent-exposed surface of the fiber. While the structure of Ac-β^3-[LIA] was determined and validated using X-ray fiber diffraction, the rigorously parameterized force field model for the β^3-peptides in various solvents can be used to determine the atomistic structure of β-peptide systems even when X-ray fiber diffraction data is not available. Furthermore, the atomistic features in the model structure can be correlated to relatively larger-scale morphological features from techniques such as AFM. The methods established in this study will be used to explore the fibril structure for other materials derived from *N*-acetylated-β^3-peptides and provide the basis for rational engineering of nano- and biomaterials.

METHODS

Preparation of Ac-β^3[LIA] fibers. The Ac-β^3[LIA] was synthesized using the solid phase peptide synthesis as previously described.[8] The peptide was dissolved in 0.2 micron filtered, milli-Q water (1mg/ml) and incubated at 37 ˚C for up to three days.

Electron microscopy. 4 μl of fiber solution (1mg/ml) in water at pH 6 was placed onto 400 mesh copper carbon/formvar coated electron microscopy grids (Agar Scientific Ltd) and allowed

to adhere before being blotted using filter paper and washed with 4 µl filtered, milliQ water. The grid was blotted and 2% w/v uranyl acetate was used to negatively stain the sample and then blotted. Dry grids were examined using a JEOL 1400 plus transmission electron microscope operated at 120 kV at 10 K and 50 K magnification.

X-ray fiber diffraction. Following incubation, 10 µl of fibrillar peptide solution (1 mg/mL in water, pH 6) was placed between two wax tipped 0.7 mm capillary tubes placed in a glass petri dish that was sealed using a parafilm to reduce evaporation and to slow alignment. Samples were allowed to air dry at room temperature to produce a partially aligned fiber sample. This method has been extensively described previously for alignment of other protein fiber samples.[61-63] Samples are air-dried but not dehydrated by this method.

The peptide fiber sample on the capillary tube was placed on a goniometer head and data were collected using a Rigaku rotating anode (CuKα) and Saturn CCD detector (Rigaku, Seven Oaks, UK), with a specimen to film distance of 100 mm and exposure times of 60 s. *CLEARER* was used to process the diffraction data to aid unit cell determination and to calculate the diffraction patterns from potential model structures arranged into potential unit cells[60] using methods previously described.[64]

Model preparation. Initial model structures of the six possible permutations of N-acetyl tripeptides comprising β^3-Leucine, β^3-Isoeucine, and β^3-Alanine: Ac-β^3[LIA], Ac-β^3[ALI], Ac-β^3[IAL], Ac-β^3[AIL], Ac-β^3[ILA], and Ac-β^3[LAI] peptide systems were adapted from the Ac-β^3[WSI] X-ray crystal structure[8] *via* a substitution of the side chains. Crystal structures of the tripeptide Ac-β^3[WSI] and hexapeptide Ac-β^3[VS$_l$LVS$_l$L] (where S$_l$ represents a β-serine modified with a linker group, see Reference 8 for more details) exhibited a nearly identical

backbone structure despite the different peptide lengths and side chains, which justifies the use of the Ac-β^3[WSI] tripeptide as template for the backbone structure of the tripeptides in this study (Figure S7). Fiber cross-sections of three to six β^3-tripeptides were prepared based on a maximization of hydrophobic groups in the fiber core with a side chain-side chain intermolecular distance of ~4 Å, while maintaining maximum solvent exposure of the C-terminal carboxyl groups. The angle between a line from the center of mass of each tripeptide and the center of mass of the group of peptides was set to 120°, 90°, 72°, and 60° for the threefold, fourfold, fivefold and sixfold radial symmetry, respectively (Figure S2). Parallel and antiparallel arrangements of the tripeptides were also examined, as well as acetyl, protonated amine, and deprotonated amine N-terminal capping. Full fibers structures were obtained by replicating the cross-section in the direction of the fiber axis of the X-ray crystal structure, in this case the *x* direction, up to 60 monomer units, resulting in a box length of up to 300 Å. The initial *y* and *z* box dimensions were both 50 Å, which was sufficient to prevent any initial periodic image interactions, and the systems were solvated using the genbox tool of GROMACS 4.6.5.[65] Equilibrated solvent boxes of methanol, ethanol, 2-propanol, chloroform, and acetone were obtained from the ATP database.[66]

Simulation details. Force field parameters for the β^3-peptides, as well as for methanol, ethanol, and chloroform, were taken from the gromos54a7beta310 force field.[67] The SPC model was used for water, and parameters for 2-propanol and acetone were taken from the ATP database.[66]

The GROMACS 4.6.5 MD code[65] was utilized for all simulations, with a non-bond interaction cutoff of 14 Å and PME treatment of long-range electrostatics. An initial energy minimization of the β^3-peptides in vacuum was performed with position restraints on the backbone heavy atoms

of 1,000 kJ mol^{-1} nm^{-2} using the steepest descent algorithm and a force tolerance of 10 kJ mol^{-1} $nm^{-1}$and maximum step size of 0.1 Å. Following solvation an additional energy minimization was performed using the same settings. The solvent and peptide side chains were equilibrated for 1 ns of NVT at 300 K with the position restraints remaining on the peptide backbone heavy atoms, followed by NPT simulation with the *x* box direction fixed and no position restraints. The temperature of the β^3-peptides was increased linearly from 1 to 300 K over the first nanosecond of the NPT simulation, while the solvent temperature was maintained at 300 K. The velocity rescale thermostat was used for all simulations, and the Berendsen barostat was used for the NPT simulations. In all simulations, bonds were constrained using the LINCS algorithm,[68] which enabled a 2 fs time-step to be used, and simulation snapshots were saved every 10 ps. Structures were characterized as "stable" when they produced a regular and consistent pattern in the direction of the fiber axis while maintaining an alpha carbon RMSD standard deviation of less than 1 Å. For the production runs, stable fibers were re-centered in a box of dimension 170 × 60 × 60 $Å^3$ and re-solvated. The initial minimization and equilibration steps were repeated, followed by pure NPT with no box constraints for 25 ns. All analysis was performed on the central ten tripeptide molecules of each strand to avoid the effects of fraying at the fiber ends. Fiber models were characterized based on diameter, solvent-accessible surface area (SASA), contact area between strands, and periodicity.

ASSOCIATED CONTENT

Supporting Information

The Supporting Information is available free of charge on the ACS Publications website at DOI:

Supporting Methods (Atomic Force Microscopy), Supporting Figures S1-S7 as described in the text (PDF)

AUTHOR INFORMATION

Corresponding Author

* E-mail: irene.yarovsky@rmit.edu.au

* E-mail: l.c.serpell@sussex.ac.uk

* E-mail: mibel.aguilar@monash.edu

Author Contributions

The manuscript was written through contributions of all authors. All authors have given approval to the final version of the manuscript. ‡These authors contributed equally.

ACKNOWLEDGMENTS

This research was undertaken with the assistance of resources from the National Computational Infrastructure (NCI), which is supported by the Australian Government, and Melbourne Bioinformatics. The authors thank Dr. Patrick Charchar for useful discussions, and the anonymous reviewers for constructive comments.

REFERENCES

1. Woolfson, D. N.; Mahmoud, Z. N. More Than Just Bare Scaffolds: Towards Multi-Component and Decorated Fibrous Biomaterials. *Chem. Soc. Rev.* **2010,** *39*, 3464-3479.

2. Hauser, C. A. E.; Zhang, S. Designer Self-Assembling Peptide Nanofiber Biological Materials. *Chem. Soc. Rev.* **2010,** *39*, 2780-2790.

3. Aida, T.; Meijer, E. W.; Stupp, S. I. Functional Supramolecular Polymers. *Science* **2012,** *335*, 813-817.

4. Seebach, D.; Beck, A. K.; Bierbaum, D. J. The World of β- and γ-Peptides Comprised of Homologated Proteinogenic Amino Acids and Other Components. *Chem. Biodiversity* **2004,** *1*, 1111-1239.

5. Gellman, S. H. Foldamers: A Manifesto. *Acc. Chem. Res.* **1998,** *31*, 173-180.

6. Wang, P. S. P.; Schepartz, A. β-Peptide Bundles: Design. Build. Analyze. Biosynthesize. *Chem. Commun.* **2016,** *52*, 7420-7432.

7. Gopalan, Romila D.; Del Borgo, Mark P.; Mechler, Adam I.; Perlmutter, P.; Aguilar, M.-I. Geometrically Precise Building Blocks: The Self-Assembly of β-Peptides. *Chem. Biol.* **2015,** *22*, 1417-1423.

8. Del Borgo, M. P.; Mechler, A. I.; Traore, D.; Forsyth, C.; Wilce, J. A.; Wilce, M. C. J.; Aguilar, M.-I.; Perlmutter, P. Supramolecular Self-Assembly of N-Acetyl-Capped β-Peptides Leads to Nano- to Macroscale Fiber Formation. *Angew. Chem., Int. Ed.* **2013,** *52*, 8266-8270.

9. Cheng, R. P.; Gellman, S. H.; DeGrado, W. F. β-Peptides: From Structure to Function. *Chem. Rev.* **2001,** *101*, 3219-3232.

10. Wu, Y.-D.; Han, W.; Wang, D.-P.; Gao, Y.; Zhao, Y.-L. Theoretical Analysis of Secondary Structures of β-Peptides. *Acc. Chem. Res.* **2008,** *41*, 1418-1427.

11. Raguse, T. L.; Lai, J. R.; LePlae, P. R.; Gellman, S. H. Toward β-Peptide Tertiary Structure: Self-Association of an Amphiphilic 14-Helix in Aqueous Solution. *Org. Lett.* **2001,** *3*, 3963-3966.

12. Hart, S. A.; Bahadoor, A. B. F.; Matthews, E. E.; Qiu, X. J.; Schepartz, A. Helix Macrodipole Control of B3-Peptide 14-Helix Stability in Water. *J. Am. Chem. Soc.* **2003,** *125*, 4022-4023.

13. Daniels, D. S.; Petersson, E. J.; Qiu, J. X.; Schepartz, A. High-Resolution Structure of a β-Peptide Bundle. *J. Am. Chem. Soc.* **2007,** *129*, 1532-1533.

14. Müller, M. M.; Windsor, M. A.; Pomerantz, W. C.; Gellman, S. H.; Hilvert, D. A Rationally Designed Aldolase Foldamer. *Angew. Chem., Int. Ed.* **2009,** *48*, 922-925.

15. Motamed, S.; Del Borgo, M. P.; Kulkarni, K.; Habila, N.; Zhou, K.; Perlmutter, P.; Forsythe, J. S.; Aguilar, M. I. A Self-Assembling β-Peptide Hydrogel for Neural Tissue Engineering. *Soft Matter* **2016,** *12*, 2243-2246.

16. Mondal, S.; Gazit, E. The Self-Assembly of Helical Peptide Building Blocks. *ChemNanoMat* **2016,** *2*, 323-332.

17. Kulkarni, K.; Motamed, S.; Habila, N.; Perlmutter, P.; Forsythe, J. S.; Aguilar, M.-I.; Del Borgo, M. P. Orthogonal Strategy for the Synthesis of Dual-Functionalised B3-Peptide Based Hydrogels. *Chem. Commun.* **2016,** *52*, 5844-5847.

18. Kwon, S.; Kim, B. J.; Lim, H.-K.; Kang, K.; Yoo, S. H.; Gong, J.; Yoon, E.; Lee, J.; Choi, I. S.; Kim, H.; Lee, H.-S. Magnetotactic Molecular Architectures from Self-Assembly of β-Peptide Foldamers. *Nat. Commun.* **2015,** *6*, 8747.

19. Luder, K.; Kulkarni, K.; Lee, H. W.; Widdop, R. E.; Del Borgo, M. P.; Aguilar, M.-I. Decorated Self-Assembling B3-Tripeptide Foldamers Form Cell Adhesive Scaffolds. *Chem. Commun.* **2016,** *52*, 4549-4552.

20. Del Borgo, M. P.; Kulkarni, K.; Tonta, M. A.; Ratcliffe, J. L.; Seoudi, R. S.; Mechler, A. I.; Perlmutter, P.; Parkington, H. C.; Aguilar, M. I. B3-Tripeptides Act as Sticky Ends to Self-Assemble into a Bioscaffold. *APL Bioengineering* **2018,** *2*, 026104.

21. Seoudi, R. S.; Del Borgo, M. P.; Kulkarni, K.; Perlmutter, P.; Aguilar, M.-I.; Mechler, A. Supramolecular Self-Assembly of 14-Helical Nanorods with Tunable Linear and Dendritic Hierarchical Morphologies. *New J. Chem.* **2015,** *39*, 3280-3287.

22. Seoudi, R. S.; Dowd, A.; Borgo, M. D.; Kulkarni, K.; Perlmutter, P.; Aguilar, M.-I.; Mechler, A. Amino Acid Sequence Controls the Self-Assembled Superstructure Morphology of N-Acetylated Tri-B3-Peptides. *Pure Appl. Chem.* **2015,** *87*, 1021–1028.

23. Daura, X.; van Gunsteren, W. F.; Rigo, D.; Jaun, B.; Seebach, D. Studying the Stability of a Helical β-Heptapeptide by Molecular Dynamics Simulations. *Chem. - Eur. J.* **1997,** *3*, 1410-1417.

24. Németh, L. J.; Hegedüs, Z.; Martinek, T. A. Predicting Order and Disorder for β-Peptide Foldamers in Water. *J. Chem. Inf. Model.* **2014,** *54*, 2776-2783.

25. Lin, Z.; van Gunsteren, W. F. Refinement of the Application of the GROMOS 54a7 Force Field to β-Peptides. *J. Comput. Chem.* **2013,** *34*, 2796-2805.

26. Glättli, A.; van Gunsteren, W. F. Are NMR-Derived Model Structures for β-Peptides Representative for the Ensemble of Structures Adopted in Solution? *Angew. Chem., Int. Ed.* **2004,** *43*, 6312-6316.

27. Trzesniak, D.; Glättli, A.; Jaun, B.; van Gunsteren, W. F. Interpreting NMR Data for β-Peptides Using Molecular Dynamics Simulations. *J. Am. Chem. Soc.* **2005,** *127*, 14320-14329.

28. Daura, X.; Gademann, K.; Schäfer, H.; Jaun, B.; Seebach, D.; van Gunsteren, W. F. The β-Peptide Hairpin in Solution: Conformational Study of a β-Hexapeptide in Methanol by NMR Spectroscopy and MD Simulation. *J. Am. Chem. Soc.* **2001,** *123*, 2393-2404.

29. Sussman, F.; Villaverde, M. C.; Estévez, J. C.; Estévez, R. J. Searching the Conformational Space of Cyclic β-Amino Acid Peptides. *J. Phys. Chem. B* **2009,** *113*, 9669-9680.

30. Huang, W.; Riniker, S.; van Gunsteren, W. F. Rapid Sampling of Folding Equilibria of β-Peptides in Methanol Using a Supramolecular Solvent Model. *J. Chem. Theory Comput.* **2014,** *10*, 2213-2223.

31. Choutko, A.; van Gunsteren, W. F. Conformational Preferences of a β-Octapeptide as Function of Solvent and Force-Field Parameters. *Helv. Chim. Acta* **2013,** *96*, 189-200.

32. Sharma, G. V. M.; Thodupunuri, P.; Sirisha, K.; Basha, S. J.; Gurava Reddy, P.; Sarma, A. V. S. Design and Synthesis of Peptides with Hybrid Helix-Turn-Helix (HTH) Motif and Their Conformational Study. *J. Org. Chem.* **2014,** *79*, 8614-8628.

33. King, N. P.; Sheffler, W.; Sawaya, M. R.; Vollmar, B. S.; Sumida, J. P.; André, I.; Gonen, T.; Yeates, T. O.; Baker, D. Computational Design of Self-Assembling Protein Nanomaterials with Atomic Level Accuracy. *Science* **2012,** *336*, 1171-1174.

34. Zhang, H. V.; Polzer, F.; Haider, M. J.; Tian, Y.; Villegas, J. A.; Kiick, K. L.; Pochan, D. J.; Saven, J. G. Computationally Designed Peptides for Self-Assembly of Nanostructured Lattices. *Sci. Adv.* **2016,** *2*, e1600307.

35. Cheng, R. P.; DeGrado, W. F. Long-Range Interactions Stabilize the Fold of a Non-Natural Oligomer. *J. Am. Chem. Soc.* **2002,** *124*, 11564-11565.

36. Yin, H.; Slusky, J. S.; Berger, B. W.; Walters, R. S.; Vilaire, G.; Litvinov, R. I.; Lear, J. D.; Caputo, G. A.; Bennett, J. S.; DeGrado, W. F. Computational Design of Peptides That Target Transmembrane Helices. *Science* **2007,** *315*, 1817.

37. Montalvo, G.; Waegele, M. M.; Shandler, S.; Gai, F.; DeGrado, W. F. Infrared Signature and Folding Dynamics of a Helical β-Peptide. *J. Am. Chem. Soc.* **2010,** *132*, 5616-5618.

38. Shandler, S. J.; Shapovalov, M. V.; Dunbrack, J. R. L.; DeGrado, W. F. Development of a Rotamer Library for Use in β-Peptide Foldamer Computational Design. *J. Am. Chem. Soc.* **2010,** *132*, 7312-7320.

39. Korendovych, I. V.; Kim, Y. H.; Ryan, A. H.; Lear, J. D.; DeGrado, W. F.; Shandler, S. J. Computational Design of a Self-Assembling β-Peptide Oligomer. *Org. Lett.* **2010,** *12*, 5142-5145.

40. Shandler, S. J.; Korendovych, I. V.; Moore, D. T.; Smith-Dupont, K. B.; Streu, C. N.; Litvinov, R. I.; Billings, P. C.; Gai, F.; Bennett, J. S.; DeGrado, W. F. Computational Design of a β-Peptide That Targets Transmembrane Helices. *J. Am. Chem. Soc.* **2011,** *133*, 12378-12381.

41. Mondal, J.; Sung, B. J.; Yethiraj, A. Sequence-Directed Organization of β-Peptides in Self-Assembled Monolayers. *J. Phys. Chem. B* **2009,** *113*, 9379-9385.

42. Mondal, J.; Zhu, X.; Cui, Q.; Yethiraj, A. Self-Assembly of β-Peptides: Insight from the Pair and Many-Body Free Energy of Association. *J. Phys. Chem. C* **2010,** *114*, 13551-13556.

43. Mondal, J.; Zhu, X.; Cui, Q.; Yethiraj, A. Sequence-Dependent Pka Shift Induced by Molecular Self-Assembly: Insights from Computer Simulation. *J. Phys. Chem. B* **2012,** *116*, 491-495.

44. Mondal, J.; Yethiraj, A. Driving Force for the Association of Amphiphilic Molecules. *J. Phys. Chem. Lett.* **2011,** *2*, 2391-2395.

45. Pizzey, C. L.; Pomerantz, W. C.; Sung, B.-J.; Yuwono, V. M.; Gellman, S. H.; Hartgerink, J. D.; Yethiraj, A.; Abbott, N. L. Characterization of Nanofibers Formed by Self-Assembly of β-Peptide Oligomers Using Small Angle X-Ray Scattering. *J. Chem. Phys.* **2008,** *129*, 095103.

46. Mondal, J.; Sung, B. J.; Yethiraj, A. Sequence Dependent Self-Assembly of β-Peptides: Insights from a Coarse-Grained Model. *J. Chem. Phys.* **2010,** *132*, 065103.

47. Mondal, J.; Yethiraj, A. Effect of Secondary Structure on the Self-Assembly of Amphiphilic Molecules: A Multiscale Simulation Study. *J. Chem. Phys.* **2012,** *136*, 084902.

48. Rathore, N.; Gellman, S. H.; de Pablo, J. J. Thermodynamic Stability of β-Peptide Helices and the Role of Cyclic Residues. *Biophys. J.* **2006,** *91*, 3425-3435.

49. Miller, C. A.; Hernández-Ortiz, J. P.; Abbott, N. L.; Gellman, S. H.; Pablo, J. J. d. Dipole-Induced Self-Assembly of Helical β-Peptides. *J. Chem. Phys.* **2008,** *129*, 015102.

50. Miller, C. A.; Gellman, S. H.; Abbott, N. L.; de Pablo, J. J. Mechanical Stability of Helical β-Peptides and a Comparison of Explicit and Implicit Solvent Models. *Biophys. J.* **2008,** *95*, 3123-3136.

51. Miller, C. A.; Gellman, S. H.; Abbott, N. L.; de Pablo, J. J. Association of Helical β-Peptides and Their Aggregation Behavior from the Potential of Mean Force in Explicit Solvent. *Biophys. J.* **2009,** *96*, 4349-4362.

52. McGovern, M.; Abbott, N.; de Pablo, Juan J. Dimerization of Helical β-Peptides in Solution. *Biophys. J.* **2012,** *102*, 1435-1442.

53. Krieger, E.; Koraimann, G.; Vriend, G. Increasing the Precision of Comparative Models with YASARA NOVA—a Self-Parameterizing Force Field. *Proteins: Struct., Funct., Bioinf.* **2002,** *47*, 393-402.

54. Fiser, A.; Šali, A. Modeller: Generation and Refinement of Homology-Based Protein Structure Models. *Methods Enzymol.* **2003,** *374*, 461-491.

55. Wood, C. W.; Bruning, M.; Ibarra, A. Á.; Bartlett, G. J.; Thomson, A. R.; Sessions, R. B.; Brady, R. L.; Woolfson, D. N. Ccbuilder: An Interactive Web-Based Tool for Building, Designing and Assessing Coiled-Coil Protein Assemblies. *Bioinformatics* **2014,** *30*, 3029-3035.

56. Ren, J. M.; Satoh, K.; Goh, T. K.; Blencowe, A.; Nagai, K.; Ishitake, K.; Christofferson, A. J.; Yiapanis, G.; Yarovsky, I.; Kamigaito, M.; Qiao, G. G. Stereospecific Cyclic Poly(Methyl Methacrylate) and Its Topology-Guided Hierarchically Controlled Supramolecular Assemblies. *Angew. Chem., Int. Ed.* **2014,** *53*, 459-464.

57. Christofferson, A. J.; Yiapanis, G.; Ren, J. M.; Qiao, G. G.; Satoh, K.; Kamigaito, M.; Yarovsky, I. Molecular Mapping of Poly(Methyl Methacrylate) Super-Helix Stereocomplexes. *Chem. Sci.* **2015,** *6*, 1370-1378.

58. Gormley, A. J.; Chandrawati, R.; Christofferson, A. J.; Loynachan, C.; Jumeaux, C.; Artzy-Schnirman, A.; Aili, D.; Yarovsky, I.; Stevens, M. M. Layer-by-Layer Self-Assembly of Polymer Films and Capsules through Coiled-Coil Peptides. *Chem. Mater.* **2015,** *27*, 5820-5824.

59. Jones, D. D. Amino Acid Properties and Side-Chain Orientation in Proteins: A Cross Correlation Approach. *J. Theor. Biol.* **1975,** *50*, 167-183.

60. Sumner Makin, O.; Sikorski, P.; Serpell, L. C. CLEARER: A New Tool for the Analysis of X-Ray Fibre Diffraction Patterns and Diffraction Simulation from Atomic Structural Models. *J. Appl. Crystallogr.* **2007,** *40*, 966-972.

61. Morris, K.; Serpell, L. From Natural to Designer Self-Assembling Biopolymers, the Structural Characterisation of Fibrous Proteins & Peptides Using Fibre Diffraction. *Chem. Soc. Rev.* **2010,** *39*, 3445-3453.

62. Morris, K. L.; Serpell, L. C. X-Ray Fibre Diffraction Studies of Amyloid Fibrils. In *Amyloid Proteins: Methods and Protocols*, E. M. Sigurdsson, M. Calero and M. Gasset, Eds. Humana Press: Totowa, NJ, 2012; pp 121-135.

63. Morris, K. L.; Chen, L.; Rodger, A.; Adams, D. J.; Serpell, L. C. Structural Determinants in a Library of Low Molecular Weight Gelators. *Soft Matter* **2015,** *11*, 1174-1181.

64. Morris, Kyle L.; Rodger, A.; Hicks, Matthew R.; Debulpaep, M.; Schymkowitz, J.; Rousseau, F.; Serpell, Louise C. Exploring the Sequence–Structure Relationship for Amyloid Peptides. *Biochem. J.* **2013,** *450*, 275.

65. Hess, B.; Kutzner, C.; van der Spoel, D.; Lindahl, E. GROMACS 4: Algorithms for Highly Efficient, Load-Balanced, and Scalable Molecular Simulation. *J. Chem. Theory Comput.* **2008,** *4*, 435-447.

66. Malde, A. K.; Zuo, L.; Breeze, M.; Stroet, M.; Poger, D.; Nair, P. C.; Oostenbrink, C.; Mark, A. E. An Automated Force Field Topology Builder (Atb) and Repository: Version 1.0. *J. Chem. Theory Comput.* **2011,** *7*, 4026-4037.

67. Huang, W.; Lin, Z.; van Gunsteren, W. F. Validation of the GROMOS 54a7 Force Field with Respect to β-Peptide Folding. *J. Chem. Theory Comput.* **2011,** *7*, 1237-1243.

68. Hess, B.; Bekker, H.; Berendsen, H. J. C.; Fraaije, J. G. E. M. LINCS: A Linear Constraint Solver for Molecular Simulations. *J. Comput. Chem.* **1997,** *18*, 1463-1472.

Table of contents entry